Raman Scattering and Phase Transition of Ammonium Nitrates

Kenji AKIYAMA,† Yoshiyuki MORIOKA, and Ichiro NAKAGAWA*

Department of Chemistry, Faculty of Science, Tohoku University, Aoba, Aramaki, Sendai 980

(Received December 15, 1980)

Polarized Raman spectra of single crystals are observed for the room-temperature phase NH_4NO_3(IV). The spectra in the low-frequency lattice vibration region as well as in the internal vibration region are well interpreted based on D_{2h}^{13} structure. Raman spectra of powdered samples are measured at various temperatures covering whole phases NH_4NO_3 I—V. A characteristic feature of Raman spectrum is clarified for each phase. An abrupt spectral change occurs in the phase transition, indicating a first order transition. The splitting of A_g and B_{1g} components of ν_3 (asymmetric stretching mode of NO_3^- ion) in NH_4NO_3 is quite large, due to the strong interionic interaction between NH_4^+ and NO_3^- ions.

In our previous paper we discussed the lattice vibrations and phase transitions of KNO_3 and $NaNO_3$ crystals.[1] In relation to the study on a series of alkali nitrates, the investigation on NH_4NO_3 is significant, from the viewpoint of the behavior of NO_3^- ion in the crystal as well as that of NH_4^+ ion. There have been several reports on the phase transition of NH_4NO_3 and it has been shown that the phase transition at high temperature is caused by the order-disorder on the rotational motion of NO_3^- ion and the following crystalline modifications exist:[2-5]

Phase I	cubic	169°C—126°C
Phase II	tetragonal	126°C— 80°C
Phase III	orthorhombic	80°C— 32°C
Phase IV	orthorhombic	32°C——18°C
Phase V	tetragonal	below −18°C

Tang and Torrie measured polycrystalline Raman spectra from room temperature down to 11 K and discussed IV⇌V phase transition.[6] James *et al.* also discussed IV⇌V phase transition as well as III⇌IV phase transition,[7] based on their Raman data measured in the temperature range 210 K—320 K. Iqbal seemed to suggest the existence of an additional phase VII,[8] for which no evidence was found by Tang and Torrie.[6] The study on the high-temperature phases by Raman measurement was made by Österlund and Rosen,[5] whose spectra seem however insufficient. Théorêt and Sandorfy measured the infrared spectra of solid crystalline films in the temperature range 169 °C——190 °C and obtained four different spectra corresponding to the I, II, IV, and VII phases.[9] In all of these studies polycrystalline samples were used for the spectral measurement and thus a definite assignment of the observed bands to the symmetry species could not be done by the polarization measurement.

We attempted a thorough spectroscopic study at various temperatures covering whole phases and clarified a characteristic feature of Raman spectrum in the low-frequency lattice vibration region for each phase. Polarized Raman spectra of single crystals were measured for the room temperature phase IV to give a characterization of the lattice vibrations. A supplementary far infrared transmission measurement was also made. We present here these results and specify how the successive phase transitions in NH_4NO_3 are reflected on the vibrational spectra.

Experimental

Single crystals of NH_4NO_3 were grown by slow evaporation of saturated aqueous solution at room temperature. Needle-like crystals of ≈5 mm length along a-axis of NH_4NO_3(IV) were obtained.

Raman spectra were recorded with a JRS 400 T triple monochromator using a standard 90° scattering configuration. The 514.5 nm line from Ar ion laser (Lexel, model 95) was used for excitation. For the measurement of polarized spectra, the natural shaped crystals were used without any polishing. At the transition temperatures these crystals cracked, probably due to the change in crystal structure, and therefore in the measurement for the high and low-temperature phases the powdered samples were employed.

Far infrared spectra were measured by a Hitachi 070 far infrared interferometer.

Crystal Structure and Factor Group Analysis

The room temperature phase IV is orthorhombic with the space group D_{2h}^{13} and two formula units per unit cell ($z=2$). The phase III is also orthorhombic but it has four formula units per unit cell and its space group is D_{2h}^{16}. The structures of these phases III and IV are sketched in Fig. 1. The low-temperature phase V is non-centric tetragonal with the space group C_4^3 and $z=8$. The high-temperature phase II is also tetragonal with the space group C_{4v}^2 and $z=2$. The phase I has a CsCl-type structure with $z=1$ in a cubic unit cell. The results of factor group analysis based on the space groups mentioned above are summarized in

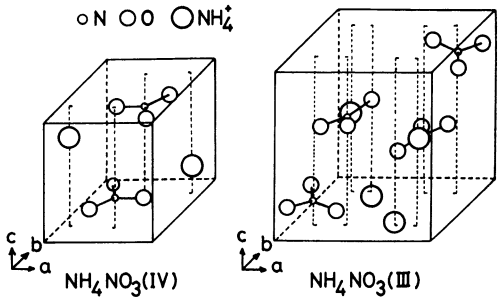

Fig. 1. Structures of NH_4NO_3(IV) and (III) crystals.

† Present address: Shin-Etsu Handotai Co., Ltd., Isobe, Annaka, Gunma 379-01.

TABLE 1. FACTOR GROUP ANALYSIS FOR NH_4NO_3 CRYSTALS[a)]

NH_4NO_3(V) ($T<-18$ °C) C_4^3 $z=8$									
C_4^3	N_t	N_a	N_o	$N_{tr.}$	$N_{ro.}$[b)]	$N_{in.}(NO_3^-)$	$N_{in.}(NH_4^+)$	Activity	
A	52	1	51	9	10(5)	12	20	c	$\alpha_{aa}+\alpha_{bb}$, α_{cc} (IR) (R)
B	52	0	52	10	10(5)	12	20		$\alpha_{aa}-\alpha_{bb}$, α_{ab} (R)
E	56	1	55	13	14(7)	12	16	(a,b)	(α_{bc}, α_{ca}) (IR) (R)
NH_4NO_3(IV) (-18 °C$<T<$32 °C) D_{2h}^{13} $z=2$									
D_{2h}^{13}	N_t	N_a	N_o	$N_{tr.}$	$N_{ro.}$[b)]	$N_{in.}(NO_3^-)$	$N_{in.}(NH_4^+)$	Activity	
A_g	9	0	9	2	0	3	4	α_{aa}, α_{bb}, α_{cc}	(R)
B_{1g}	8	0	8	2	2(1)	2	2	α_{ab}	(R)
B_{2g}	7	0	7	2	2(1)	1	2	α_{ac}	(R)
B_{3g}	3	0	3	0	2(1)	0	1	α_{bc}	(R)
A_u	3	0	3	0	2(1)	0	1		
B_{1u}	7	1	6	1	2(1)	1	2	c	(IR)
B_{2u}	8	1	7	1	2(1)	2	2	b	(IR)
B_{3u}	9	1	8	1	0	3	4	a	(IR)
NH_4NO_3(III) (32 °C$<T<$80 °C) D_{2h}^{16} $z=4$									
D_{2h}^{16}	N_t	N_a	N_o	$N_{tr.}$	$N_{ro.}$[b)]	$N_{in.}(NO_3^-)$	$N_{in.}(NH_4^+)$	Activity	
A_g	16	0	16	4	2(1)	4	6	α_{aa}, α_{bb}, α_{cc}	(R)
B_{1g}	11	0	11	2	4(2)	2	3	α_{ab}	(R)
B_{2g}	16	0	16	4	2(1)	4	6	α_{ac}	(R)
B_{3g}	11	0	11	2	4(2)	2	3	α_{bc}	(R)
A_u	11	0	11	2	4(2)	2	3		
B_{1u}	16	1	15	3	2(1)	4	6	c	(IR)
B_{2u}	11	1	10	1	4(2)	2	3	b	(IR)
B_{3u}	16	1	15	3	2(1)	4	6	a	(IR)
NH_4NO_3(II) (80 °C$<T<$126 °C) C_{4v}^5 $z=2$									
C_{4v}^5	N_t	N_a	N_o	$N_{tr.}$	$N_{ro.}$	$N_{in.}(NO_3^-)$		Activity	
A_1	5	1	4	1	0	3	c	$\alpha_{aa}+\alpha_{bb}$, α_{cc}	(IR) (R)
A_2	2	0	2	1	1	0			
B_1	4	0	4	1	0	3		$\alpha_{aa}-\alpha_{bb}$	(R)
B_2	1	0	1	0	1	0		α_{ac}	(R)
E	9	1	8	3	2	3	(a,b)	(α_{bc},α_{ca})	(IR) (R)

a) N_t; total freedom, N_a; acoustic modes, N_o; optical active modes, $N_{tr.}$; translational lattice modes, N_{ro}; rotational lattice modes, $N_{in.}(NO_3^-)$; internal modes of NO_3^-, $N_{in.}(NH_4^+)$; internal modes of NH_4^+, (R); Raman active modes. (*IR*); infrared active modes. b) Values in parentheses denote the rotational freedom of NH_4^+ ions.

Table 1. No Raman active mode exists for the structure of the phase I.

Results and Discussion

Low frequency Lattice Vibration. In this region we may expect primarily the rotational and translational lattice modes of NO_3^- ion. The rotational modes of NH_4^+ ion are expected in the region higher than 300 cm^{-1}.[10] The polarized Raman spectra below 300 cm^{-1} at room temperature are shown in Fig. 2, which arise from the phase IV. The observed frequencies and assignments to the symmetry species based on D_{2h}^{13} structure are listed in Table 2. In the spectra of powdered sample shown in Fig. 3, three bands around 90 cm^{-1}, 140 cm^{-1}, and 170 cm^{-1} are observed at 29 °C, which correspond to the three intense bands at 85 cm^{-1} (B_{2g}), 139 cm^{-1} (B_{2g}), and 170 cm^{-1} (B_{3g}), respectively, observed in the polarized spectra. On referring to Table 1, the 170 cm^{-1} band (B_{3g}) is unambiguously

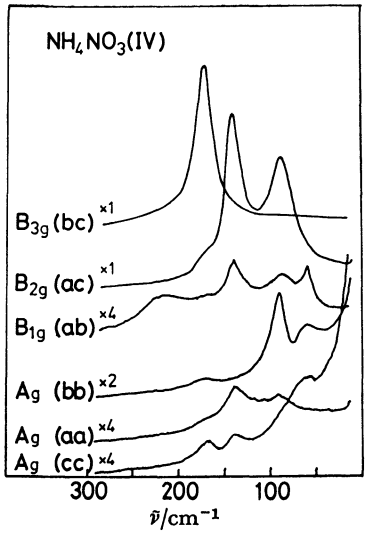

Fig. 2. Polarized Raman spectra of NH_4NO_3(IV) crystal in the low-frequancy lattice vibration region.

Table 2. Observed frequencies in cm^{-1} of NH_4NO_3[a)]

NH_4NO_3(V) IR (77 K)	NH_4NO_3(V) R (77 K)	NH_4NO_3(V) R[b)] (11 K)		NH_4NO_3(IV) IR	NH_4NO_3(IV) R (room temperature)		NH_4NO_3(III) R (32 °C)	NH_4NO_3(II) R (81 °C)
43	48	49	$T(NO_3^-)$		58(B_{1g})	$T_b(NO_3^-)$		≈ 60
65	61	62					58(B_{2g}) $T_{ac}(NO_3^-)$	
69	73	75			60(A_g)	$T_a(NO_3^-)$		
78	85	84					68(A_g) $T_{ac}(NO_3^-)$	
89		87			85(B_{2g})	$T_c(NO_3^-)$		
102	98	96					100(A_g) $R_b(NO_3^-)$	
104		98			90(A_g)	$T_a(NO_3^-)$		≈120
	110	112	$R(NO_3^-)$					
119	135	135			139(B_{2g})	$R_b(NO_3^-)$	128(B_{1g}, B_{3g}) $R_a(NO_3^-)$	
140	138	140						
160	161	162			170(B_{3g})	$R_a(NO_3^-)$		
190	189	185						
		191						
	201	203	$T(NH_4^+)$					
		207		≈200	220(B_{1g})	$T_c(NH_4^+)$		
≈240	230	231						
		245						
	709	726	ν_4	717	715(A_g, B_{1g})	ν_4	715 ν_4	710
	728						717	722
			ν_2	830		ν_2		
	1057		ν_1	1046	1043(A_g)	ν_1	1050 ν_1	1050
	1288	1321	ν_3	≈1350	1289(A_g)	ν_3	1320 ν_3	
	1389	1406			1415(B_{1g})		≈1355	
	1415		ν_4'	1450	1418(A_g)	ν_4'	≈1410 ν_4'	
					1461(B_{1g})			
	1419	1427	ν_3					
	1447	1451						
	1458							

a) T and R denote translational and rotational lattice modes, respectively. ν_1—ν_4: internal modes of NO_3^- ion. ν_4': internal mode of NH_4^+ ion. b) Observed values by Tang and Torrie.[6)]

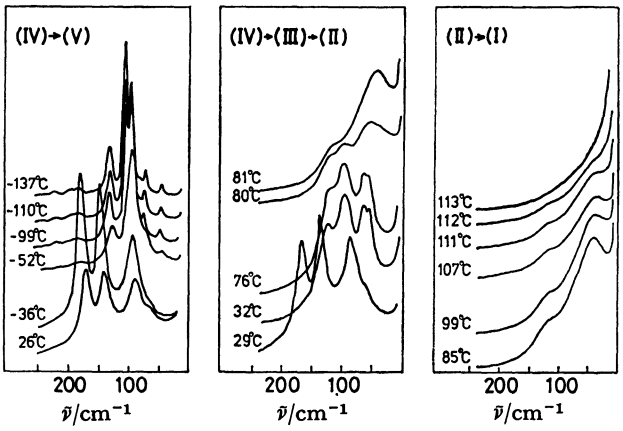

Fig. 3. Raman spectra of powdered samples at various temperatures in the low-frequency region.

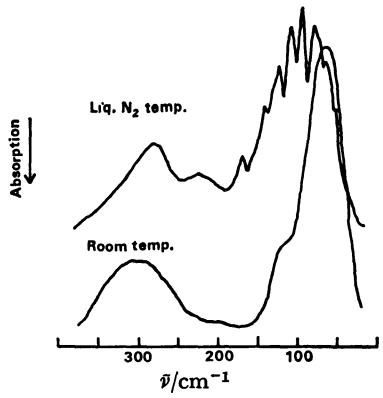

Fig. 4. Far infrared transmission spectrum of NH_4NO_3-(IV) (Nujol mull). This spectrum is recorded by the single-beam operation. The low transmissivity around 0 and 400 cm^{-1} is due to the efficiency of the beam-splitter.

assigned to the rotational lattice mode of NO_3^- ion about a-axis, while the 85 cm^{-1} (B_{2g}) and 139 cm^{-1} (B_{2g}) bands are assigned to the translational mode along c-axis and the rotational mode about b-axis, which are more or less coupled with each other. The B_{1g} rotational lattice mode about c-axis might be very weak since the polarizability does not change singnificantly for the rotation about an axis perpendicular to the NO_3 plane.

Other four weak bands 58 cm^{-1} (B_{1g}), 60 cm^{-1} (A_g), 90 cm^{-1} (A_g), and 220 cm^{-1} (B_{1g}) observed in the polarized spectra are assigned to the translational lattice modes. Among them the 220 cm^{-1} (B_{1g}) band is associated with the NH_4^+ translational mode, since in the Raman spectrum of KNO_3 no band is observed

around 200 cm^{-1}. Furthermore in the far infrared transmission spectrum shown in Fig. 4 a broad band around 200 cm^{-1} is observed, which also exists in the far infrared spectrum of NH_4Cl.

The Raman spectra at various temperatures in Fig. 3 reveal an abrupt spectral change in the phase transition as expected for a first order transition. This can be seen more clearly in the frequency change with temperature shown in Fig. 5.

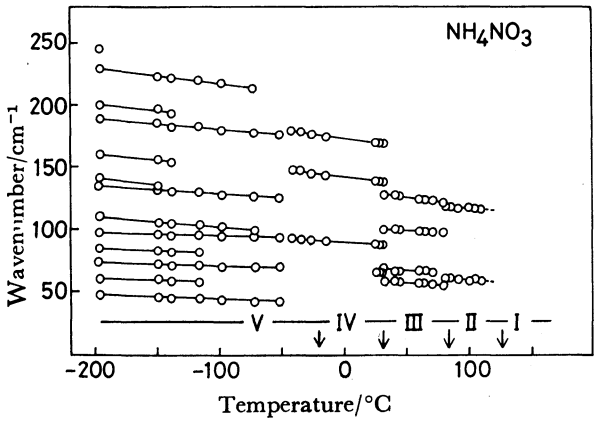

Fig. 5. Temperature dependence of Raman frequencies in NH_4NO_3.

First we discuss the spectra of high-temperature phases. Österlund and Rosen showed in their Raman spectra the phase III was not observed but the phase IV was converted directly to the phase II at 50 °C.[5] In our measurement the spectrum at 81 °C in Fig. 3(b) is considered to arise from the phase II. However, in the temperature range 32 °C—80 °C we have the spectrum which is different from those of both phase II and IV and this corresponds to the spectrum of phase III. The spectrum of phase III is also confirmed by the single crystal spectrum of NH_4NO_3–KNO_3 mixed crystal which takes the same structure as NH_4NO_3-(III).[11]

In the spectrum of phase II two bands are observed. As the temperature is raised these bands shift to lower frequency and show no anomalous behavior as the II→I transition is approached. Actually at 113 °C no band is observed. In the phase I, NO_3^-, and NH_4^+ groups are freely rotating and are described to have a spherical symmetry, resulting in the CsCl-type structure of NH_4NO_3(I). No Raman band is observed as expected from this structure.

Next we discuss the spectra of the low-temperature phase V. As seen in Figs. 3 and 5, an abrupt spectral change corresponding to the phase transition IV⇌V is observed around −50 °C, which is lower than the generally accepted temperature −18 °C. Probably a supercooling state is produced. The cooling rate in our measurement is ≈0.5 K/min. Our measurement is made down to 77 K but no evidence is found for another low-temperature phase VII. Our result at 77 K is in agreement with that at 11 K by Tang and Torrie,[6] who also could not find phase VII.

Table 2 summarizes the observed frequencies in various phases.

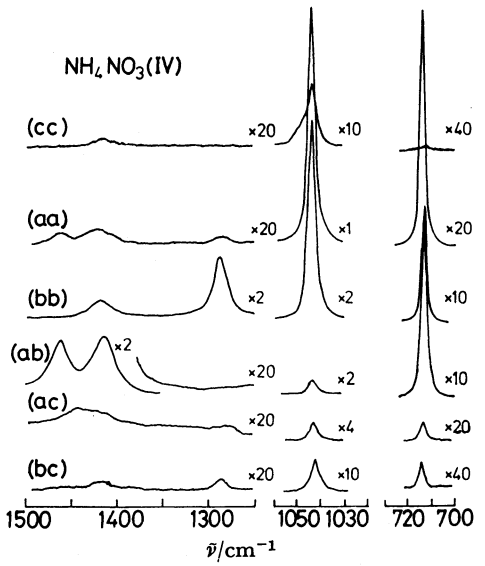

Fig. 6. Polarized Raman spectra of NH_4NO_3(IV) crystal in the internal vibration region.

Internal Vibrations of NO_3^- and NH_4^+ Ions. The polarized Raman spectra in the internal vibration region at room temperature are shown in Fig. 6, which can be interpreted based on D_{2h}^{13} crystal symmetry. The correlation between the D_{3h} (NO_3^- free ion) and the D_{2h}^{13} (NH_4NO_3 crystal) is as follows:

	$D_{3h}(NO_3^-$ ion)	C_{2v}(site sym.)	$D_{2h}^{13}(NH_4NO_3)$
A_1'	ν_1(≈1050 cm^{-1})	A_1	A_g+B_{3u}
A_2''	ν_2(≈ 830 cm^{-1})	B_2	$B_{2g}+B_{1u}$
E'	ν_3(≈1350 cm^{-1})	A_1	A_g+B_{3u}
	ν_4(≈ 720 cm^{-1})	B_1	$B_{1g}+B_{2u}$

As for NH_4^+ ion the following correlation exists:

	$T_d(NH_4^+$ ion)	C_{2v}(site sym.)	$D_{2h}^{13}(NH_4NO_3)$
A_1	ν_1'	A_1	A_g+B_{3u}
E	ν_2'	A_1	A_g+B_{3u}
		A_2	$B_{3g}+A_u$
F_2	ν_3'	A_1	A_g+B_{3u}
		B_1	$B_{1g}+B_{2u}$
	ν_4'(≈1450 cm^{-1})	B_2	$B_{2g}+B_{1u}$

In the spectra of Fig. 6, the 1043 cm^{-1} band (ν_1 : A_g) and the 715 cm^{-1} band (ν_4 : A_g) are observed as expected from the correlation diagram. The 715 cm^{-1} band is also observed in the (ab) scattering configuration, which corresponds to the $\nu_4(B_{1g})$.

In the region 1250 cm^{-1}—1500 cm^{-1}, the ν_3 of NO_3^- ion and ν_4' of NH_4^+ ion are expected. On referring to the correlation diagram, the 1289 cm^{-1} and 1418 cm^{-1} bands observed in the (bb) configuration are assigned to the $\nu_3(A_g)$ and $\nu_4'(A_g)$ respectively, and the 1415 cm^{-1} and 1461 cm^{-1} bands observed in the (ab) configuration are assigned to the $\nu_3(B_{1g})$ and $\nu_4'(B_{1g})$ respectively.

The splitting of the A_g and B_{1g} components of the ν_3 (asymmetric stretching mode of NO_3^- ion) in NH_4NO_3-(IV) is 126 cm^{-1}, which seems abnormally large

compared with $\approx 10\ cm^{-1}$ in KNO_3(II). In NH_4NO_3-(III) this splitting is $\approx 35\ cm^{-1}$ (see Table 2). In the NH_4NO_3–KNO_3 mixed crystals $(NH_4)_xK_{1-x}NO_3$ which will be discussed in the following paper, the ν_3 splitting is $\approx 40\ cm^{-1}$. The large splitting of ν_3 may be caused by the strong interionic interaction between NH_4^+ and NO_3^- ions. The neutron diffraction measurement by Choi *et al.* showed that in NH_4NO_3(IV) the hydrogen bond is formed between the hydrogen in NH_4^+ ion and one of the oxygens in NO_3^- ion.[12] This kind of hydrogen bond also exists in NH_4NO_3(V), which gives rise to the large splitting of ν_3 in the low-temperature phase V as observed by Tong and Torrie.[6] A crystallographic study suggests that the phase transition III⇌IV is related to the hydrogen bonding, which is reflected on the splitting of ν_3. James *et al.* suggested that the bands at $1289\ cm^{-1}$ and $1415\ cm^{-1}$ are the transverse and longitudinal components of ν_3 and the structure of phase IV is non-centric due to the observation of such a polar mode in the Raman spectrum.[7] However, their interpretation is highly unlikely since as seen in Fig. 6 polarized Raman spectra of single crystals for various scattering configurations do not reveal any TO/LO character and they can be interpreted based on D_{2h}^{13} structure as mentioned before.

In conclusion, the structural change can be sensitively probed by studying the Raman active lattice modes in the low-frequency region. An abrupt spectral change occurs in the phase transition, indicating a first order transition. The spectra of single crystals for the room-temperature phase IV, in the low-frequency region as well as in the internal vibration region, are reasonably interpreted based on D_{2h}^{13} structure.

A part of this investigation was supported by a grant of Yamada Science Foundation.

References

1) K. Akiyama, Y. Morioka, and I. Nakagawa, *J. Phys. Soc. Jpn.*, **48**, 898 (1980).
2) M. Nagatani, T. Seiyama, M. Sakiyama, H. Suga, and S. Seki, *Bull. Chem. Soc. Jpn.*, **40**, 1833 (1967).
3) R. N. Brown and A. C. Mclaren, *Proc. R. Soc. London, Ser. A*, **266**, 329 (1962).
4) S. B. Hendricks, E. Posnjak, and F. C. Kracek, *J. Am. Chem. Soc.*, **54**, 2766 (1932).
5) K. Österlund and H. J. Rosen, *Solid State Commun.*, **15**, 1355 (1974).
6) M. C. Tang and B. H. Torrie, *J. Phys. Chem. Solids*, **39**, 845 (1977).
7) D. W. James, M. T. Carrick, and W. H. Leong, *Chem. Phys. Lett.*, **28**, 117 (1974).
8) Z. Iqbal, *Chem. Phys. Lett.*, **40**, 41 (1976).
9) A. Théorêt and C. Sandorfy, *Can. J. Chem.*, **42**, 57 (1964).
10) J. R. Durig and D. J. Antion, *J. Chem. Phys.*, **51**, 3639 (1969).
11) J. R. Holden and C. W. Dickinson, *J. Phys. Chem.*, **79**, 249 (1975).
12) C. S. Choi, J. E. Mapes, and E. Prince, *Acta Crystallogr., Sect. B*, **28**, 1357 (1972).